Chaos

Quint points lattice in a driven Belousov–Zhabotinsky reaction model

Cite as: Chaos **31**, 053124 (2021); https://doi.org/10.1063/5.0047167
Submitted: 10 February 2021 . Accepted: 03 May 2021 . Published Online: 19 May 2021

Richard J. Field, Joana G. Freire, and Jason A. C. Gallas

Chaos ARTICLE scitation.org/journal/cha

Quint points lattice in a driven Belousov–Zhabotinsky reaction model

Cite as: Chaos **31**, 053124 (2021); doi: 10.1063/5.0047167
Submitted: 10 February 2021 · Accepted: 3 May 2021 ·
Published Online: 19 May 2021

View Online Export Citation CrossMark

Richard J. Field,[1,a] Joana G. Freire,[2,3,b] and Jason A. C. Gallas[3,4,c]

AFFILIATIONS

[1] Department of Chemistry, University of Montana, Missoula, Montana 59812, USA
[2] Instituto Dom Luiz, Universidade de Lisboa, 1749-016 Lisboa, Portugal
[3] Instituto de Altos Estudos da Paraíba, 58039-190 João Pessoa, Brazil
[4] Complexity Sciences Center, 9225 Collins Ave. Suite 1208, Surfside, Florida 33154, USA

[a] **Electronic mail:** richard.field@mso.umt.edu
[b] **Electronic mail:** jcfreire@fc.ul.pt
[c] **Author to whom correspondence should be addressed:** jason.gallas@gmail.com

ABSTRACT

We report the discovery of a regular lattice of exceptional *quint points* in a periodically driven oscillator, namely, in the frequency–amplitude control parameter space of a photochemically periodically perturbed ruthenium-catalyzed Belousov–Zhabotinsky reaction model. Quint points are singular boundary points where five distinct stable oscillatory phases coalesce. While spikes of the activator show a smooth and continuous variation, the spikes of the inhibitor show an intricate but regular branching into a myriad of stable phases that have fivefold contact points. Such boundary points form a wide parameter lattice as a function of the frequency and amplitude of light absorption. These findings revise current knowledge about the topology of the control parameter space of a celebrated prototypical example of an oscillating chemical reaction.

A version of the oscillatory Belousov–Zhabotinsky reaction catalyzed by ruthenium ion is photosensitive. We report here high-resolution computational stability diagrams obtained for an oscillatory perturbation $I(t) = a\sin(\omega t)$ of this nonlinear system, recorded in the (ω, a) plane. The calculated oscillatory trajectories appear with different numbers of spikes in $Ru(phen)_3^{3+}$ (the inhibitory species) per period. Trajectories with an equal number of spikes cluster in certain areas that correlate to a regular adding-doubling complexification route. The remarkable feature of these areas is that in multiple cases (a lattice), five distinct areas join at an exceptional point (ω, a), which we refer to as a quint point. We conjecture such points to be generic properties observable in complex oscillatory systems. We expect lattices of quint points to be detected experimentally.

I. INTRODUCTION

Nonlinear oscillators are well-known generators of intricate wave patterns.[1–5] For instance, stable periodic oscillations may display phenomena such as doubling and adding cascades. As control parameters are continuously changed, waveforms often change by acquiring more and more spikes (local maxima), and it is therefore natural to inquire how spikes emerge distributed in phase diagrams as a function of internal control parameters or external perturbations. This is a basic and quite difficult question due to the total absence of a proper theoretical framework to predict analytically the dynamics of even simple models governed by nonlinear differential equations. The characterization of the possible waveforms produced by nonlinear oscillators is a problem of interest to all scientific disciplines and applied sciences.

Bifurcation phenomena involving the variation of just a single parameter are reasonably well understood.[1–5] In contrast, only fragmentary information is available for situations requiring the simultaneous variation of two or more independent control parameters. The difficulty lies in drawing a plethora of phase boundaries delimiting oscillations with distinct waveforms and number of spikes per period, and in determining phase volume and relative orientation in phase diagrams. Fortunately, high-performance high-throughput computer clusters, outperforming by wide margins

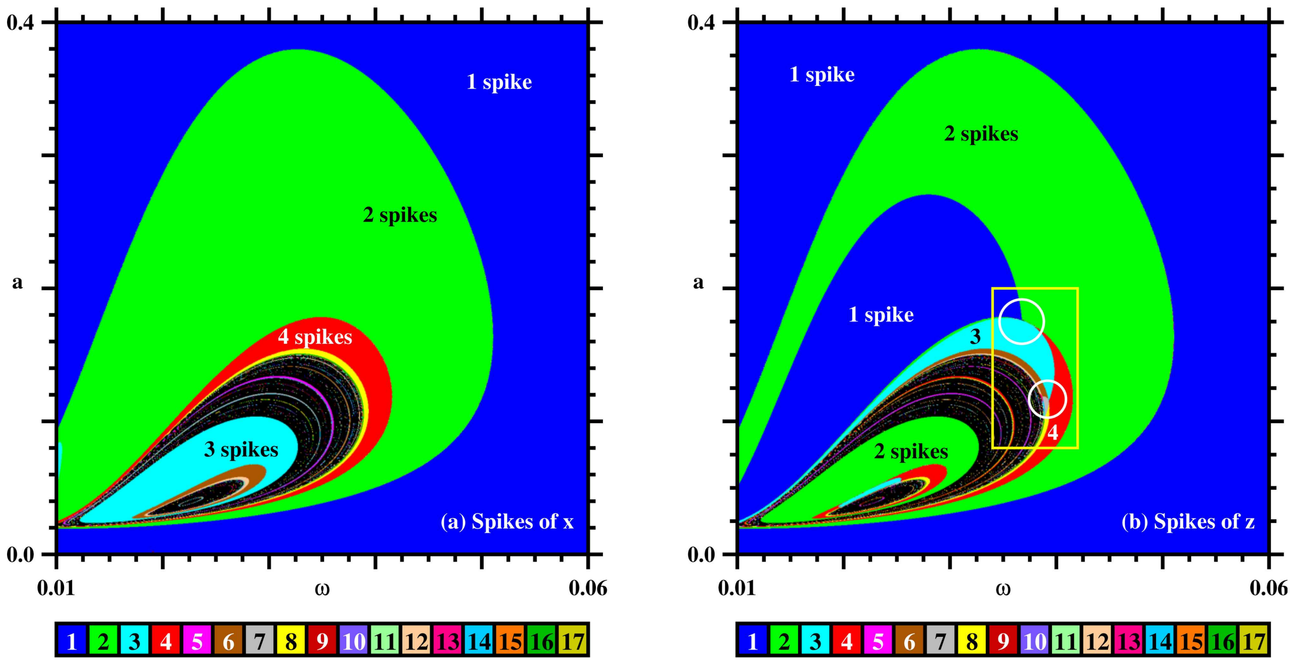

FIG. 1. Frequency–amplitude stability phase diagrams obtained by counting spikes per period of (a) activator *x* and (b) inhibitor *z*. Colors represent the number of spikes per period, as indicated in the colorbar. Black denotes parameters leading to non-periodic (chaotic) oscillations. The first two quint points of the lattice are located at the center of the circles in (b). The rectangular box is shown magnified in Fig. 2.

everything previously available, allow access to such invaluable cartographic information about complex systems.

Our aim here is to report the discovery of a wide lattice of exceptional parameter points, quint points, recorded in the frequency–amplitude control parameter space of a periodically driven ruthenium-catalyzed Belousov–Zhabotinsky reaction. Each quint point of the lattice functions as a waveform "access custodian:" starting from any quint point, slight parameter deviations from them allow one to change, to select, a specific waveform from a set of five distinct stable patterns that coalesce at the quint point, each waveform characterized by a different number of spikes per period. Examples of such quint points and the five phases coalescing on them may be seen in Figs. 1(b), 2(b), and 2(d). Therefore, oscillations in nonlinear systems continue to surprise and marvel.

II. THE RUTHENIUM-CATALYZED REACTION

The Belousov–Zhabotinsky (BZ) reaction[6] is the prototype of a chemical reaction governed by a nonlinear dynamic law and exhibits oscillations in the concentrations of intermediate species. It is the only chemical system that exhibits sustained, autonomous oscillations in a batch reactor. In the classic BZ reaction, the driving chemical reaction is the oxidation of malonic acid $[CH_2(COOH)_2]$ by a bromate ion (BrO_3^-) in aqueous 1M H_2SO_4. The direct reaction between BrO_3^- and malonic acid is very slow, and it is typically catalyzed by a redox couple consisting of two metal ions separated by a single electron, e.g., Ce(III)/Ce(IV) in the classic recipe, or by similar couples, e.g., $Fe(phen)_3^{2+}$/ $Fe(phen)_3^{3+}$ and $Ru(phen)_3^{2+}$/ $Ru(phen)_3^{3+}$ with phen ≡ phenanthroline. The Ru-catalyzed system[7] is interesting because it can be perturbed via light absorption by $Ru(phen)_3^{2+}$ to yield the excited species $Ru^*(phen)_3^{2+}$, which eventually leads to the generation of Br^-, the species that controls the BZ oscillations. This photochemically perturbed system is the system studied here.

Field, Körős, and Noyes (FKN)[8] described the BZ chemical mechanism in 1972 as consisting of nine reactions involving eight intermediates. This mechanism has very largely stood the test of time.[6,9] Field and Noyes[10] used rate-determining step approximations to reduce the FKN mechanism to a system of three variables: $[HBrO_2]$, $[Br^-]$, and [Ce(IV)], that together define the dynamic structure of the BZ reaction. The scaled kinetic equations form the so-called Oregonator model, namely,

$$\varepsilon \frac{dx}{dt} = x(1-x) + y(q-x),$$
$$\sigma \frac{dy}{dt} = \eta z - y(q+x), \qquad (1)$$
$$\frac{dz}{dt} = x - z.$$

The dimensionless parameters ε, σ, and q contain information about the rate equations of the five irreversible steps of the reduced mechanism and the concentrations of malonic acid. Typical values are $\sigma \ll \varepsilon, q \ll 1$. The time scales of x and y are similar and both are much faster than z. Thus, it is possible to reduce Eq. (1) to two variables either by causing x to follow y (set $dx/dt = 0$) or by causing

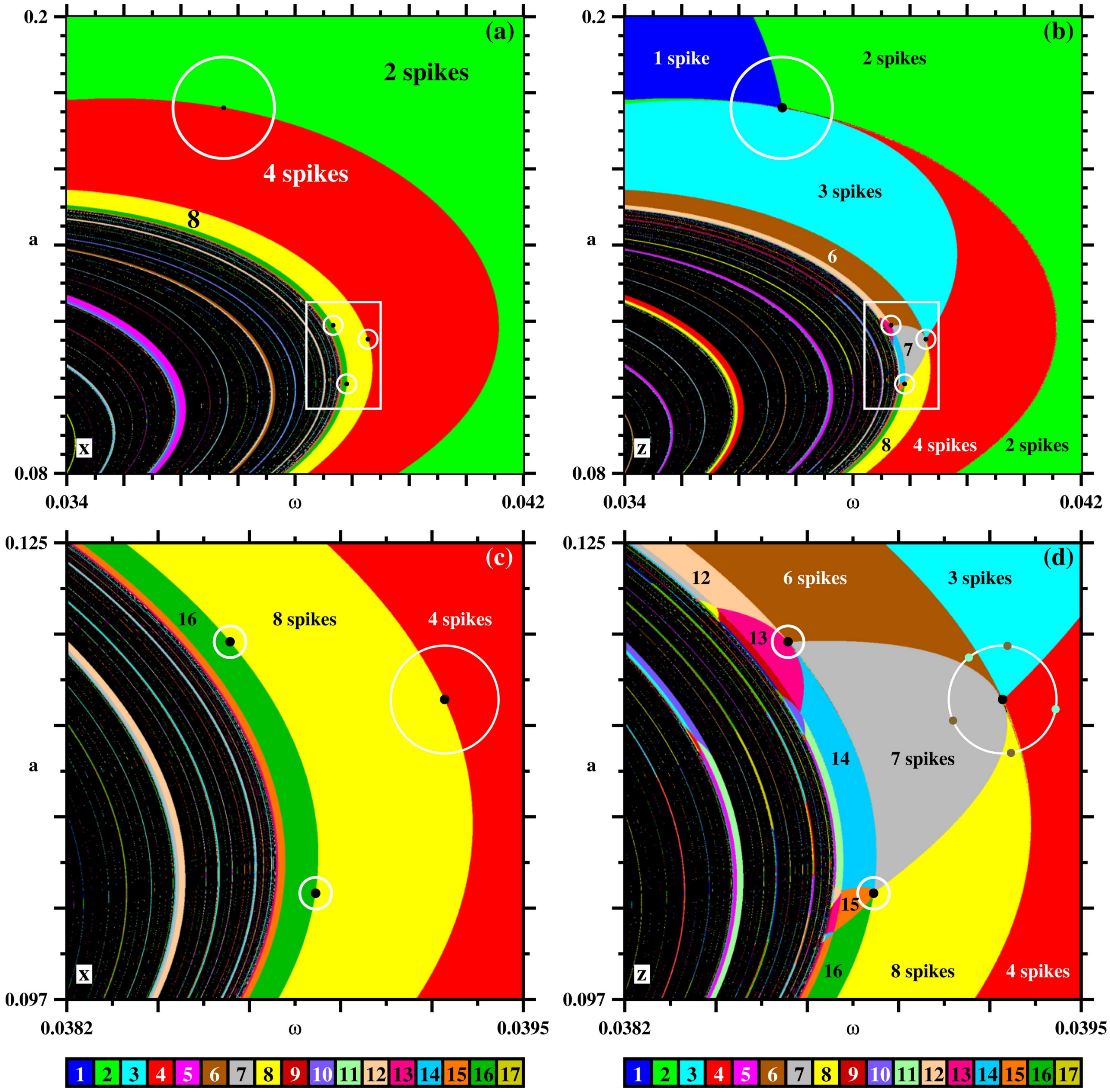

FIG. 2. Marked differences between the spikes of activator x (left column) and of inhibitor z (right column). For reference, circles and points are also added in panels (a) and (c). (b) The first four quint points, recorded by counting spikes of z, are located at the center of the circles. Quint points are vertices of parabolic arcs. New quint points emerge at both extremities of every parabolic arc. Numbers refer to the number of spikes of individual phases of periodic oscillations. Black denotes the phases of chaos, i.e., lack of periodicity. (d) Magnification of the box in (b) showing the next few *generations* of quint points at the vertices of the parabolas with $13 = 6 + 7$ and $15 = 7 + 8$ spikes. The generic unfolding is illustrated schematically in Fig. 3. Coordinates of the five points around the larger circle are given in Fig. 4.

y to follow x (set $dy/dt = 0$). Tyson[11] and Tyson and Fife[12] showed that y is a little faster than x (and the result less complex) and set $dy/dt = 0$ obtaining thereby $y = \eta z/(q + x)$. The photosensitivity of the Ru-catalyzed BZ reaction allows an opportunity to investigate its behavior under external, periodic, light-perturbation $I(t)$ that is simply added to the activator (autocatalytic, here x) equation, with little regard to the actual chemistry occurring, following the previous work by Español and Rotstein[13] in this journal. Therefore, after simple rescaling $z \leftarrow \eta z$ and $t \leftarrow t/\varepsilon$, the model becomes

$$\frac{dx}{dt} = \frac{1}{10}\left[x(1-x) + \frac{q-x}{q+x}z + I(t)\right], \tag{2}$$

$$\frac{dz}{dt} = \frac{\varepsilon}{10}(\eta x - z), \tag{3}$$

where $I(t) = a\sin(\omega t)$ is an external periodic perturbation with amplitude a and frequency ω.

Following the literature,[13] we fix $q = 0.1$, $\varepsilon = 0.025$, and $\eta = 5$ and investigate the dynamics as a function of ω and a.

III. COMPUTING STABILITY DIAGRAMS

A popular tool to explore dynamical systems is the Lyapunov exponent,[14] which is used to sort out periodic from chaotic oscillations.[1,2,4,5] However, the computational cost to obtain Lyapunov diagrams is relatively high, and their very naive two-phases classification is far from the maximal possible. Considerably richer cartographic information is provided by the so-called *isospike diagrams*,[15–26] which use distinct colors to codify chaos and the number of spikes (local maxima) per period of the periodic oscillations. In this simple and less costly way, one obtains diagrams that perfectly reproduce the Lyapunov classification but contain a significant enhancement: instead of lumping together all periodic oscillations into a single phase as Lyapunov diagrams do, isospike diagrams display explicitly the number of spikes of each individual oscillation. For a survey regarding stability diagrams, see Ref. 19.

The individual stability diagrams in Figs. 1 and 2 cover parameter windows of interest with grids of $1200 \times 1200 = 1.44 \times 10^6$ equidistant points. For each point, the temporal evolution of the reaction is computed by integrating numerically Eqs. (2) and (3) with the standard fourth-order Runge–Kutta algorithm, using a fixed time step $h = 0.02$. For each row, integrations start at the rightmost boundary from an arbitrary initial condition $(x, z) = (0.16, 1.16)$ and proceed horizontally to the left by *following the attractor*, namely, by re-using the last computed values of x and z to start a new integration after decreasing ω. The first 0.4×10^6 integration steps were discarded as transient time needed to approach the attractor, with the subsequent 8×10^6 steps used to compute up to 800 extrema (maxima and minima) for both variables, and then checking whether or not spikes repeated.

IV. A LATTICE OF QUINT POINTS

Figure 1 shows stability diagrams displaying the variation of the number of spikes per period of activator x and inhibitor z using a 17 color palette. Oscillations with more than 17 spikes are represented by recycling the 17 basic colors "modulo 17," namely, by assigning to them the color index obtained as the remainder of the integer division of the number of spikes by 17. Here, multiples of 17 are assigned the index 17. Black is used to represent the lack of numerically detectable periodicity, "chaos." From Fig. 1(b), one recognizes that the spikes of inhibitor z display a rich and regular variation when the frequency and amplitude of the external oscillating light beam change.

Figure 2 shows isospike stability diagrams for both variables x and z in a magnified view of the box in Fig. 1. From Figs. 2(a) and 2(b), it is easy to recognize the smooth variation of the spikes. In contrast, on the upper part of Fig. 2(b), there are two large phases, characterized by periodic oscillations with one and with two spikes per period, which are separated by a smooth boundary. As a decreases along this separation boundary, one eventually reaches the first quint point of the lattice, indicated by the black dot at the center of a circle. At this quint point, the number of spikes suddenly trifurcates producing three new phases. The largest and more easily visible is a large parabolic-like phase characterized by periodic oscillations with three spikes, the sum of the spikes of the two phases preceding it: $3 = 1 + 2$ spikes. In addition to this parabolic phase, there are two cuspidal-like phases meeting at the quint point, characterized by two and four spikes per period. The cuspidal four-spikes phase fanning out to the right of the quint point is easy to recognize. To the left of the quint point, there is a two-spikes cuspidal phase that, however, is too compressed to be identified in the scale of the figure but may be easily identified on suitable magnifications (not shown here). This narrow phase fans out to the left of $\omega = 0.034$. It results from a spikes-doubling transition of the one-spike phase above it. Analogously, the four-spikes phase is a spikes-doubling transition of the two-spikes phase immediately above it.

In Fig. 2(b), there is a curious asymmetry for ω decreasing when one moves leftward from the two-spikes phase on the right: On the top part of the diagram, there is a *decreasing* $1 \leftarrow 2$ transition, while an *increasing* $4 \leftarrow 2$ transition occurs on the lower part of the figure. The rich mosaic of phases in Fig. 2 cannot be discovered from Lyapunov diagrams because, as already mentioned, such diagrams lump together all periodic oscillations into a single phase (color), washing out all the information contained in the spikes of the oscillations.

Figure 2(d), a magnification of the box in Fig. 2(b), shows the next phase-trifurcation leading to phases with 6, 7, and 8 spikes per period and two new quint points at the ends of the parabolic phase of 7 spikes. Such points are located at the center of the circles and, as before, mark phase trifurcations leading to phases with 12, 13, 14, 15, and 16 spikes, as indicated by different colors. The phases with 12 and 16 spikes result from spikes-doubling transitions from the phases with 6 and 8 spikes on their right. Analogously, a 14-spikes phase results from the spikes-doubling of the phase with seven spikes. However, there are also spikes-adding phases, namely, the two new parabolic arcs with $13 = 6 + 7$ and $15 = 7 + 8$ spikes. As indicated by the colors, such intricate but regular adding-doubling cascading continues, with subsequent phases getting more and more difficult to visualize very quickly.

In Fig. 2(d), it is possible to recognize that the several stripes of periodic oscillations embedded in chaos also show color changes along them, a clear sign of the presence of regular adding-doubling complexification cascades in them too. The regular unfolding of the adding-doubling complexification cascading observed in Fig. 2 is summarized schematically in Fig. 3.

In hindsight, the differences seen between the stability diagrams in Figs. 1(a) and 1(b) or between the two columns in Fig. 2 should not be totally unexpected. In the same way as a three-dimensional attractor looks different when represented by distinct two-dimensional phase-space projections, two-dimensional parameter sections display distinct aspects of the underlying

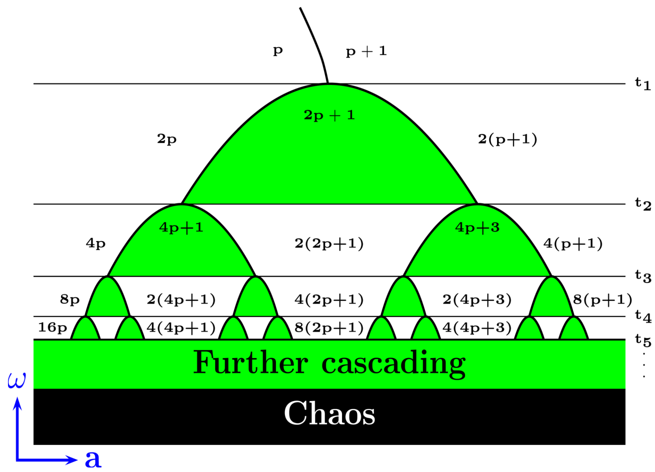

FIG. 3. Schematic representation of the regular adding-doubling complexification cascading observed in Fig. 2. All parabolic phases contain phases with odd number of spikes, while their adjacent phases have even number of spikes. The adding-doubling complexification cascade is apparently finite and not very long. Adapted from Ref. 18.

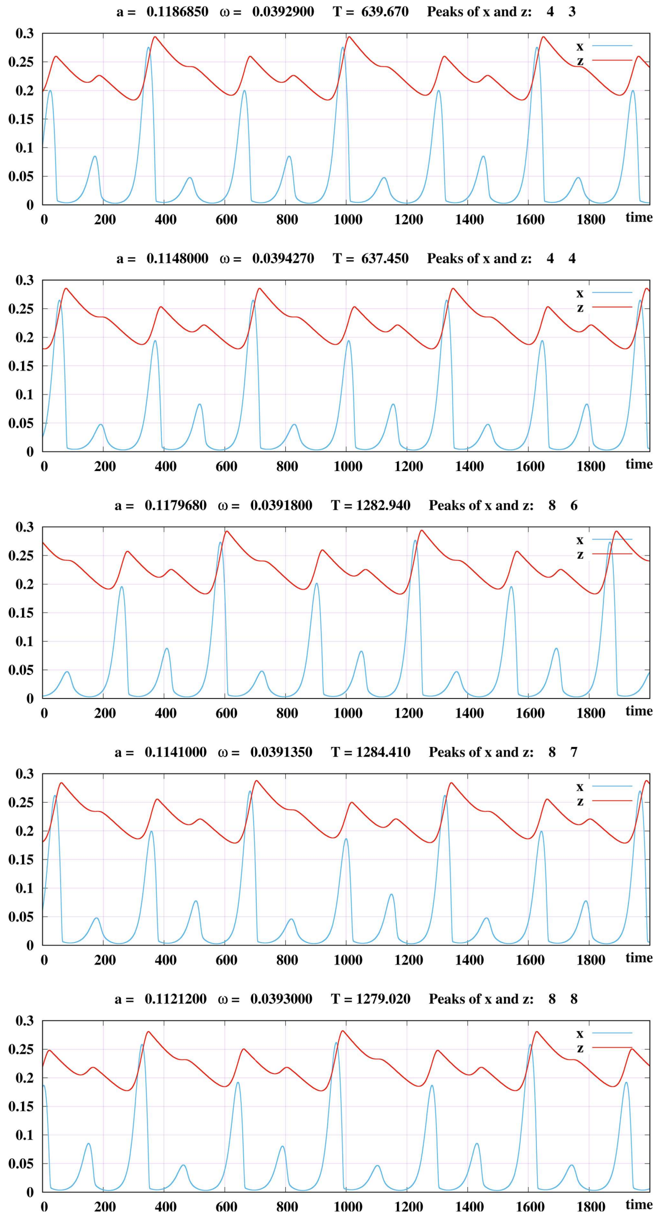

FIG. 4. Temporal evolution of activator x and inhibitor z for the five points distributed around the circle in Fig. 2(d). The period T varies with amplitude a and frequency ω, but it is always the same for both x and z.

multidimensional control parameter space when inspected with different dynamical variables.

What happens to the waveform of the oscillations as the adding-doubling cascade proceeds? The answer is given in Fig. 4 that shows waveforms for x and z at five points marked around the larger circle in Fig. 2(d). The individual panels of Fig. 4 record the (a, ω) coordinates of the points, the corresponding period of the oscillations, as well as the number of spikes of x and z. Small spike differences are difficult to identify in the scale of Fig. 4 but are visible in magnifications (not shown). Noteworthy is the fact that by doubling the period of oscillations seen in the topmost panel, one obtains $2 \times 639.670 = 1279.340$, which is close to the period 1279.020 recorded for the oscillations in the panel at the bottom. In contrast, $2 \times 637.450 = 1274.900$ that is not close to any of the other two periods 1282.940 and 1284.410 in the figure. This emphasizes the fact that, for any fixed set of parameters, the *period* measured using any variable of the model is always the same, independently of the number of spikes that the variable may have. It also emphasizes the fact that the phenomena described here are connected with the *discrete* variation of the number of spikes, not with the *continuous* variation of the period. Thus, inside every parabolic arc, one finds spike-adding, not period-adding.

V. CONCLUSION

This work reports the discovery of an intricate but regular adding-doubling complexification cascading in a driven Belousov–Zhabotinsky reaction. It significantly extends and complements previous findings of Español and Rotstein[13] published in this journal. The complexification cascading is observed in the frequency–amplitude control plane of the reaction and is summarized schematically in Fig. 3. This regular complexification route illustrates the unexpected intricacy and beauty of the behavior of a periodically perturbed nonlinear system and revises knowledge about the topology of the control space of a prototypical oscillating chemical reaction. The predicted model oscillations have not yet been observed experimentally but are within reach. Furthermore, we hypothesize the adding-doubling cascading reported here to be a generic property of complex oscillatory systems, not difficult to observe experimentally in other contexts.

ACKNOWLEDGMENTS

J.G.F. was supported by FCT, Portugal, Project No. UIDB/50019/2020-IDL. J.A.C.G. was partially supported by CNPq, Brazil, under Grant No. 305305/2020-4. All bitmaps were computed at the CESUP-UFRGS Supercomputer Center of the Federal University in Porto Alegre, Brazil.

DATA AVAILABILITY

Data sharing is not applicable to this article as no new data were created or analyzed in this study.

REFERENCES

[1]D. B. Forger, *Biological Clocks, Rhythms, and Oscillations* (MIT Press, Cambridge, 2017).
[2]J. Argyris, G. Faust, M. Haase, and R. Friedrich, *An Exploration of Dynamical Systems and Chaos*, 2nd ed. (Springer, Berlin, 2015).
[3]S. H. Strogatz, *Nonlinear Dynamics and Chaos: With Applications to Physics, Biology, Chemistry, and Engineering*, 2nd ed. (Westview Press, Boulder, 2015).
[4]I. R. Epstein and J. A. Pojman, *An Introduction to Nonlinear Chemical Dynamics: Oscillations, Waves, Patterns, and Chaos* (Oxford University Press, Oxford, 1998).
[5]R. J. Field and L. Györgyi, *Chaos in Chemistry and Biochemistry* (World Scientific, Singapore, 1993).
[6]A. M. Zhabotinsky, Scholarpedia **2**(9), 1435 (2007).
[7]R. Toth and A. Taylor, "The tris(2,2′-bipyridyl) ruthenium-catalyzed Belousov–Zhabotinsky reaction," Prog. React. Kinet. Mech. **31**, 59–115 (2006).
[8]R. J. Field, E. Körös, and R. M. Noyes, "Oscillations in chemical systems II. Thorough analysis of temporal oscillation in the bromate-cerium-malonic acid system," J. Am. Chem. Soc. **94**, 8649–8664 (1972).
[9]A. F. Taylor, "The Belousov–Zhabotinsky reaction," Prog. React. Kinet. Mech. **27**, 247–325 (2002).
[10]R. J. Field and R. M. Noyes, "Oscillations in chemical systems IV. Limit cycle behavior in a model of a real chemical reaction," J. Chem. Phys. **60**, 1877–1884 (1974).
[11]J. J. Tyson, "A quantitative account of oscillations, bistability, and traveling waves in the Belousov–Zhabotinsky reaction," in *Oscillations and Traveling Waves in Chemical Systems*, edited by R. J. Field and M. Burger (Wiley-Interscience, New York, 1985).
[12]J. J. Tyson and P. C. Fife, "Target patterns in a realistic model of the Belousov–Zhabotinsky reaction," J. Chem. Phys. **73**, 2224–2237 (1980).
[13]M. I. Español and H. G. Rotstein, "Complex mixed-mode oscillatory patterns in a periodically forced excitable Belousov–Zhabotinsky reaction model," Chaos **25**, 064612 (2015).
[14]A. Pikovsky and A. Politi, *Lyapunov Exponents: A Tool to Explore Complex Dynamics* (Cambridge University Press, Cambridge, 2016).
[15]J. G. Freire and J. A. C. Gallas, "Stern-Brocot trees in the periodicity of mixed-mode oscillations," Phys. Chem. Chem. Phys. **13**, 12191–12198 (2011).
[16]M. A. Nascimento, J. A. C. Gallas, and H. Varela, "Self-organized distribution of periodicity and chaos in an electrochemical oscillator," Phys. Chem. Chem. Phys. **13**, 441–446 (2011).
[17]J. G. Freire, T. Pöschel, and J. A. C. Gallas, "Stern-Brocot trees in spiking and bursting of sigmoidal maps," Europhys. Lett. **100**, 48002 (2012).
[18]M. R. Gallas, M. R. Gallas, and J. A. C. Gallas, "Distribution of chaos and periodic spikes in a three-cell population model of cancer," Eur. Phys. J. Spec. Top. **233**, 2131–2144 (2014).
[19]J. A. C. Gallas, "Spiking systematics in some CO_2 laser models," Adv. At. Mol. Opt. Phys. **65**, 127–191 (2016).
[20]X. B. Rao, Y. D. Chu, L. Xu, Y. X. Chang, and J. G. Zhang, "Fractal structures in centrifugal flywheel governor system," Commun. Nonlinear Sci. Numer. Simul. **50**, 330–339 (2017).
[21]L. Xu, Y. D. Chu, and Q. Yang, "Novel dynamical scenario of the two-stage Colpitts oscillator," Chaos, Solitons Fractals **138**, 109998 (2020).
[22]X. B. Rao, X. P. Zhao, J. S. Gao, and J. G. Zhang, "Self-organization with fast-slow time scale dynamics in a memristor-based Shinriki's circuit," Commun. Nonlinear Sci. Numer. Simul. **94**, 105569 (2021).
[23]J. A. C. Gallas, M. J. B. Hauser, and L. F. Olsen, "Complexity of a peroxidase-oxidase reaction model," Phys. Chem. Chem. Phys. **23**, 1943–1955 (2021).
[24]J. A. C. Gallas, "Overlapping spikes cascades in a semiconductor laser proxy," Brazilian J. Phys. (published online).
[25]J. A. Vélez, J. Bragard, L. M. Pérez, A. M. Cabanas, O. J. Suarez, D. Laroze, and H. L. Mancini, "Periodicity characterization of the nonlinear magnetization dynamics," Chaos **30**, 093112 (2020).
[26]C. S. Rodrigues, C. G. P. dos Santos, C. C. de Miranda, E. Parma, H. Varela, and R. Nagao, "A numerical investigation of the effect of external resistence and applied potential on the distribution of periodicity and chaos in the anodic dissolution of nickel," Phys. Chem. Chem. Phys. **22**, 21823–21834 (2020).